1B4-5

A Modified Holographic Technique for Antenna Measurements and Object Imaging

[#]Mark Leach, Sergei Skobelev, Michael J Fdo, Michael Elsdon, David Smith
School of Computing, Engineering and Information Sciences, Northumbria University
Ellison Building, Newcastle upon Tyne, NE1 8ST, UK, m.leach@unn.ac.uk

1. Introduction

The application of the holographic technique to the measurement of antenna fields and to the imaging of objects has been documented in [1] and [2]. In antenna near-field measurements, the holographic technique avoids use of the expensive vector analyser usually required to obtain the necessary amplitude and phase data directly, as only simple power measurements are needed. With respect to object imaging, microwaves are being employed in an increasing range of applications from medical imaging, in which it has specific use in early stage breast cancer detection [3], to airport security personnel scanners [4]. Holography is attractive in these areas due to its ability to reduce system cost, producing three-dimensional images from scalar measurements. One of the key trade-offs in opting for the holographic scalar measurement, is the increase in the number of samples required to obtain sufficient term separation in the hologram processing, as detailed in [1]. This paper details some modifications to the measurement system, which offer an improved utilisation of hologram spectral width and offer the possibility to reduce the over-sampling previously required. The paper is organised as follows, Section 2 provides the theoretical background to the modified holographic technique. Section 3 presents a comparison of practical and simulation results obtained for a medium-gain antenna. Section 4 shows results obtained for the imaging of simple metal targets and conclusions are drawn in Section 5.

2. Modified Holographic Theory and System

The planar holographic technique involves the recording of the interference pattern (hologram) formed between two coherent waves, the object wave (E_O) and a well-known reference wave (E_R), over a planar aperture. Ideally the reference wave is planar with controllable phase. The interference (I) between the two waves over a plane in located in x, y can be written as:

$$I^{+}(x,y) = \left|E_R(x,y) + E_O(x,y)\right|^2 = \left(\left|E_R\right|^2 + \left|E_O\right|^2\right) + E_R^{*} \cdot E_O + E_R \cdot E_O^{*} \qquad (1)$$

Where E_R has uniform magnitude and a linear phase component over the surface varying in either x or y or both. The field of the object wave can be recovered via the Fourier Transform (FT). It can be seen by the substitution of such a reference wave into (1), that the consequent FT will yield a spectrum with the three distinct regions. The two bracketed magnitude terms will be located at the origin of the spectrum while the other two components will appear re-centred at $\pm k_r$, which represents the linear phase gradient of the reference wave. Providing the overlap between the significant component regions is negligible, then the spectral component relating to $E_R^{*}E_O$ can be filtered from the spectrum, centred at the spectral origin and the Inverse FT applied to obtain the original object field E_O scaled by the reference magnitude.

For the measurement of high gain antenna where the spectral width of E_O is narrow, the separation of the three terms in the hologram spectrum can be achieved using the maximum possible sample spacing of $\lambda/2$ limited by the Nyquist theorem. In the case of medium gain antenna it has been shown previously in [1] that separation can still be achieved but at the cost of decreasing the sample spacing, i.e. significantly increasing the number of samples and hence the acquisition and processing time. A modified system topology from that applied previously is shown in Figure 1.

ISBN: 978-4-88552-223-9 C3055©IEICE

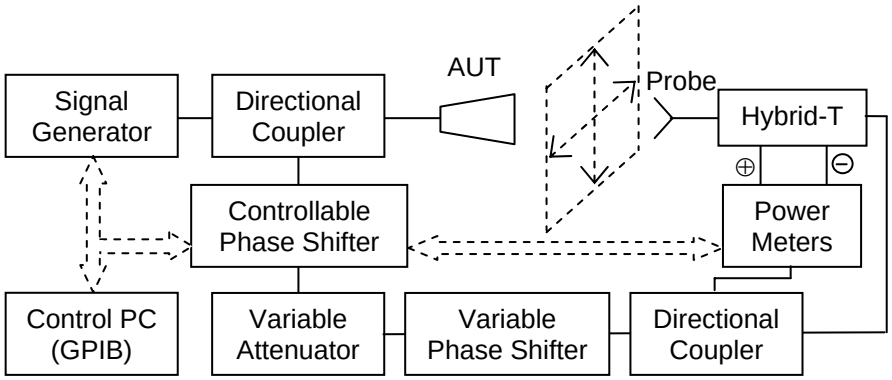

Figure 1: Modified Holographic System Topology

Two additional measurements are made at each sample location in the modified approach. Firstly the power at the difference port of the hybrid-T, previously terminated in a matched load, and secondly the power in a coupled portion of the reference wave. The Intensity recorded at the output of the difference port is given by:

$$I^{-}(x,y) = \left|E_R - E_O\right|^2 = \left(\left|E_R\right|^2 + \left|E_O\right|^2\right) - E_R^{*} \cdot E_O - E_R \cdot E_O^{*} \tag{2}$$

The subtraction of (2) from (1) leads to:

$$I_{\Delta}(x,y) = I^{+}(x,y) - I^{-}(x,y) = 2\left(E_R^{*} \cdot E_O + E_R \cdot E_O^{*}\right) \tag{3}$$

From (3) it can be seen that the two bracketed magnitude terms in (1) and (2), located at the origin of the spectrum of (1) have been removed and only the two components containing the object field and its conjugate remain. As a result it is only necessary to obtain separation of two components, which can be achieved through the use of larger sample spacing. Figure 2 shows a comparison of the FT's of (1) and (3), using the field of a medium gain pyramidal horn antenna as the object field. To obtain the necessary separation in (1) a sample spacing Δ_x of $\lambda/6$ with a reference phase of $k_r\Delta_x=2\pi/3$, whilst in (3) the same level of separation can be achieved using $\lambda/4$ sample spacing and $k_r\Delta_x=\pi/2$. As part of the processing the average intensity value has been removed in the case of (1) and zero buffering has been applied in both cases for spectral smoothing.

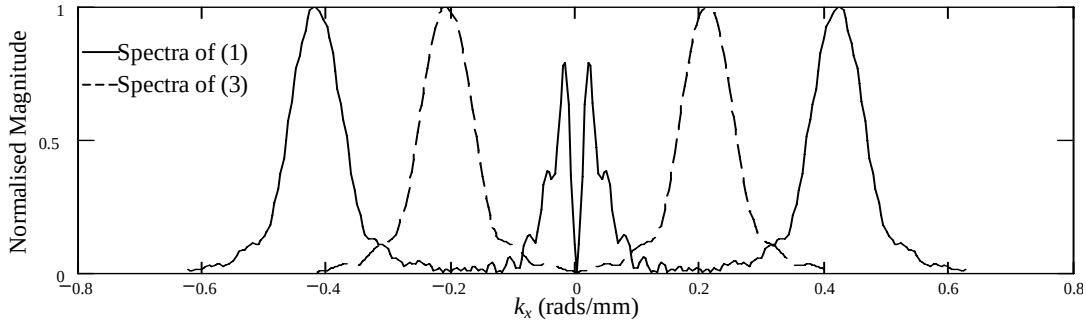

Figure 2: Comparison of Spectra of (1) and (3)

Ideally, the magnitude of the reference wave applied to the input of the hybrid T is constant for all phase changes applied to the controllable phase shifter, however in practice small variations occur as the phase is changed. As a result of this variation the convolution operation between E_O and E_R in the FT provides a new challenge. Measurement of the reference power from the directional coupler allows the variation to be divided out.

On obtaining the spectrum of the object field further processing can be performed to attain images of the field at different planes using the back propagation theory as described in [1]. For antenna measurements this provides a means of obtaining images of antenna aperture fields, useful in fault diagnosis. Similarly in object imaging, where the object field is derived from a target object under illumination, a microwave image of the object can be found by performing the back propagation process at multiple distances until a focussed object image is attained.

3. Antenna Measurement

Using the system in Figure 1 near-field measurements have been made for the medium-gain Flann 16240 X-Band pyramidal horn with dimensions h=79 mm (E-Plane), w=109 mm and l=240 mm. The measurements were collected at 10 GHz over a 900×900 mm plane located at a distance of 100 mm from the antenna, samples were spaced at $\lambda/6$ in the x axis and $\lambda/2$ in the y axis, with a reference phase increment of $2\pi/3$ radians per sample in the x axis. At each location x, y all three power measurements are collected and saved to the PC. Post processing of the measurements involves obtaining the result of (3), followed by zero buffering and the FT. Upon filtering the object field spectrum, the antenna far-field radiation pattern can be attained. Direct magnitude and phase measurements have also been collected using the NSI 2000 planar scanning system. Probe compensation has been applied to both sets of measurements utilising the same probe coefficients derived from the NSI 2000 software. Figure 3 shows a comparison of the principal planes obtained from the two measurements and those predicted by performing an aperture integration using model number 4 given in [5].

The sample spacing has been chosen to offer the same degree of separation as in previous work, since it was found through investigation that the subtraction in (3) did not provide a spectrum of only two components. The non ideal hybrid-T used does not provide an equal power division between the E and H Plane ports and therefore the magnitude terms in (1) and (2) do not cancel.

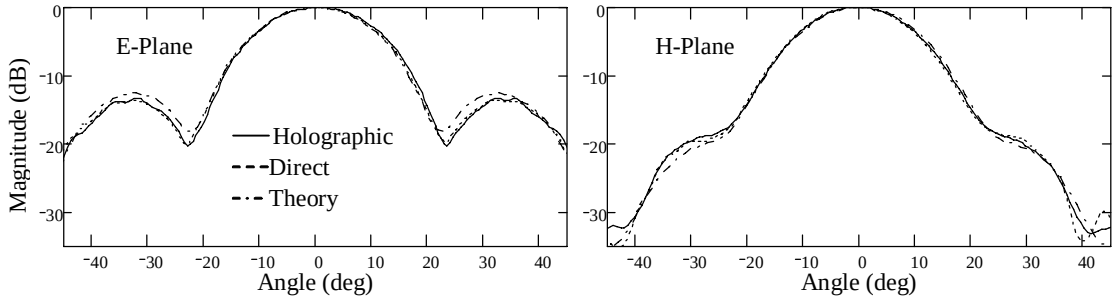

Figure 3: Comparison of Experimental and Calculated Radiation Patterns

The planes are shown over the measurement valid angle, given as the angle from the edge of the horn to the edge of the measurement plane. The two measurement techniques show a very high level of agreement over the valid angle region. However, it is seen that the theoretical model does not accurately predict the far-field distribution, especially in the E-Plane side lobes. It is suggested that this is due to the inaccuracy of the aperture field modelled, as it does not account for aperture field amplitude variation resulting from the flare of the pyramidal horn.

4. Object Imaging

To apply the system in Figure 1 to object imaging, the AUT must be replaced by an illuminating source aimed at a target object and the probe positioned as to intersect the scattered field. Ideally, the object should be continuously illuminated by a plane wave from a fixed source; however problems arise in locating the source so that there is no blockage by the probe antenna. In place of the fixed source, a circulator is connected to the probe, allowing the probe to be used as both illuminator and receiver. The k_z component of the wave vector used to perform the back

propagation is different to that used in antenna measurements as the as the wave has travelled twice the distance to the object, this is described in [4].

A flat rectangular metal object with dimensions equal to that of the pyramidal horn aperture mounted on wood was scanned using the same dimensions used in the measurement of the pyramidal horn. After processing the data as previously described and performing the back propagation using the appropriate k_z vector component followed by the Inverse FT the magnitude and phase of the field obtained in the plane of the object are shown in Figure 4.

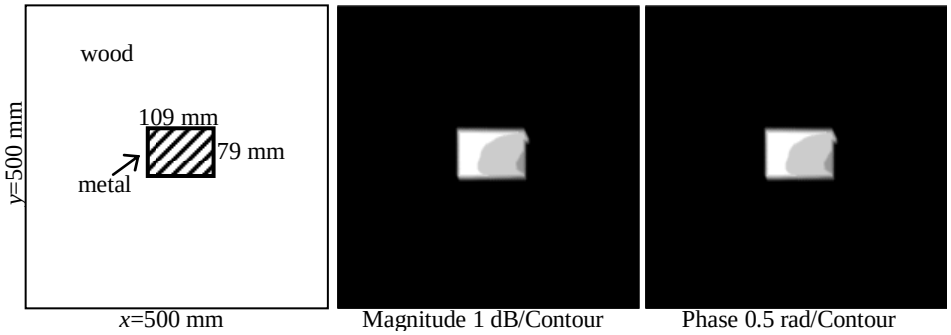

Figure 4: Magnitude and Phase Images of Metallic Object

The reconstructed field in the object plane shown in Figure 4 appears well focussed in both the magnitude and phase images and of the same size as the original object. From the phase image it is seen that there is a phase shift across the object, which can be attributed to the experimental setup and the object being placed at an angle to the measurement plane. This would also account for the change in magnitude across the object.

5. Conclusions

A modified approach to the synthetic reference holographic measurement technique that utilises two additional scalar measurements has been described. It has been shown how this approach could lead to a reduction in the number of samples required for the measurement of a medium gain pyramidal horn antenna. Initial antenna measurement results have been presented and have been shown to provide comparable results to those obtained via direct amplitude and phase measurements. The ability to reconstruct amplitude and phase images of a simple object using the modified approach has also been shown. The problem associated with the non-ideal hybrid-T could be solved in future work through consideration of the T's matching coefficients.

References

[1] D. Smith, M. Leach, M. Elsdon and S. J. Foti, "Indirect holographic techniques for determining antenna radiation characteristics and imaging aperture fields", IEEE Antennas & Propagation Magazine, vol. 37, no. 3, June 2007.

[2] M. Leach, M. Elsdon, S. J. Foti and D. Smith, "Imaging Dielectric Objects Using A Novel Synthetic Off-Axis Holographic Technique", Microwave and Optical Technology Letters, vol. 48, no. 10, pp. 1957-1961, Oct. 2006.

[3] M. Elsdon, M. Leach, M. J. Fdo, S. J. Foti and D. Smith, "Early stage breast cancer detection using indirect microwave holography", Proc. 36th European Microwave Conf., Manchester, UK, vol. 1, pp. 1256-1259, Sept. 2006.

[4] D. Sheen, D. McMakin and T. Hall, "Three-dimensional millimeter-wave imaging for concealed weapon detection" IEEE Trans. Microwave Theory and Techniques, vol. 49, no. 9, pp. 1581-1592, Sept. 2001.

[5] G. Mayhew-Ridgers, J. W. Odendaal and J. Joubert, "On primary incident wave models for pyramidal horn gain calculations", IEEE Trans. Antennas Propag., vol. 48, no. 8, pp. 1246-1252, Aug. 2000.